Preequilibrium Asymmetries in the ^{239}Pu(n,f) Prompt Fission Neutron Spectrum

K. J. Kelly, T. Kawano, J. M. O'Donnell, J. A. Gomez, M. Devlin, D. Neudecker, P. Talou, A. E. Lovell, M. C. White, R. C. Haight, T. N. Taddeucci, S. M. Mosby, H. Y. Lee, C. Y. Wu, R. Henderson, J. Henderson, and M. Q. Buckner

Phys. Rev. Lett. **122**, 072503 — Published 22 February 2019

DOI: 10.1103/PhysRevLett.122.072503

Pre-Equilibrium Asymmetries in the ^{239}Pu(n,f) Prompt Fission Neutron Spectrum

K. J. Kelly[1a], T. Kawano[1], J. M. O'Donnell[1], J. A. Gomez[1], M. Devlin[1], D. Neudecker[1], P. Talou[1], A. E. Lovell[1], M. C. White[1], R. C. Haight[1], T. N. Taddeucci[1], S. M. Mosby[1], H. Y. Lee[1], C. Y. Wu[2], R. Henderson[2], J. Henderson[2], M. Q. Buckner[2]

[1] *Los Alamos National Laboratory, Los Alamos, NM 87545, USA*

[2] *Lawrence Livermore National Laboratory, Livermore, CA 94550, USA*

(Dated: January 9, 2019)

The physical properties of neutrons emitted from neutron-induced fission are fundamental to our understanding of nuclear fission. However, while state-of-the-art fission models still incorporate isotropic fission neutron spectra, it is believed that the pre-equilibrium pre-fission component of these spectra is strongly anisotropic. The lack of experimental guidance on this feature has not motivated incorporation of anisotropic neutron spectra in fission models, though any significant anisotropy would impact descriptions of a fissioning system. In the present work, an excess of counts at high energies in the fission neutron spectrum of ^{239}Pu is clearly observed and identified as an excess of the pre-equilibrium pre-fission distribution above the post-fission neutron spectrum. This excess is separated from the underlying post-fission neutron spectrum and its angular distribution is determined as a function in incident neutron energy and outgoing neutron detection angle. Comparison with neutron scattering models provides the first experimental evidence that the pre-equilibrium angular distribution is uncorrelated with the fission axis. The results presented here also impact the interpretation of several influential prompt fission neutron spectrum measurements.

PACS numbers: 25.40.Lw,26.20.Cd,27.30.+t

[a] Corresponding Author

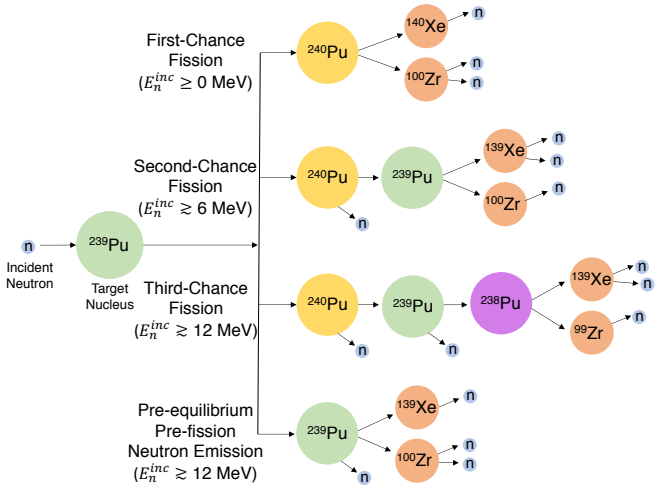

FIG. 1: (color online) An illustration of the reaction paths accessible to a ^{239}Pu + n system undergoing nuclear fission, with the incident neutron energies, E_n^{inc}. The fission fragments shown represent typical fragments emitted from the corresponding fissioning nucleus, though their precise identity as well as the number of neutrons emitted from each nucleus are arbitrarily chosen. See the text for a discussion.

Models of nuclear fission reflect our understanding of the fission process. These models are used to inform nuclear data evaluations, which are then used to predict the performance of nuclear systems and reactors [1–3]. Despite the obvious need for a complete understanding of the fission process, we are only just now beginning to experimentally observe fundamental features of fission relating to the neutrons emitted during the fission process. Neutron-induced fission can proceed via a number of possible reaction paths depending on the incident neutron energy, the most important of which for the present work are illustrated in Fig. 1. For ^{239}Pu, fission can follow the capture of a neutron and equilibration of the compound nucleus for all incident neutron energies, in which case a ^{240}Pu nucleus fissions ("first-chance fission"; first row of Fig. 1). At higher incident energies, one or more pre-fission neutrons can be emitted following equilibration of the compound nucleus and before fission occurs if it is energetically allowed. If a single pre-fission neutron is emitted ("second-chance fission"; second row of Fig. 1), then the resulting ^{239}Pu nucleus can fission. It is the energy spectrum of the neutrons emitted promptly following nuclear fission that is commonly referred to as the prompt fission neutron spectrum (PFNS). However, the pre-fission neutrons shown in Fig. 1 cannot be separated from the acquired neutron spectra because pre-fission neutrons are absorbed and re-emitted on a timescale that is fast compared to the onset of fission.

The details of multi-chance fission are not well known and are estimated from models with incomplete experimental validation [2–4]. A particularly unknown feature of second-chance fission is the transition from equilibrium pre-fission neutron emission to pre-equilibrium pre-fission neutron emission (illustrated in the bottom row of Fig. 1) and the corresponding angular distributions of these pre-equilibrium pre-fission neutrons. As opposed to second-chance fission where an equilibrated compound nucleus is formed prior to pre-fission neutron emission, in fission preceded by emission of a pre-equilibrium neutron the *incident* neutron undergoes an inelastic scattering reaction with the target nucleus and leaves the reacting system before a compound nucleus is formed (i.e., before nuclear equilibrium can be established). Neutron scattering theory predicts that pre-equilibrium pre-fission neutrons will have an angular distribution that is enhanced at forward angles with respect to the momentum direction of the incident neutron [5], which would have a significant impact on the directional neutron flux within a fissioning system. Pre-equilibrium neutron emission angles are also expected to be uncorrelated with the fission axis. Given the lack of experimental data on this PFNS feature, nuclear data evaluations typically use a model intended to predict the *energy distribution* of the pre-equilibrium PFNS component, but without any prediction of the *angular distribution* [5]. Experimental determination of the correlation or absence of correlation with the fission axis would be essential for fission modeling efforts.

Pre-equilibrium pre-fission neutrons have been observed to exist for ^{232}Th, ^{235}U, and ^{238}U neutron-induced fission [6–10], but no continuous double-differential (i.e., continuously divided as a function of incident neutron energy as well as outgoing neutron energy and detection angle) measurement to determine the angular distributions of

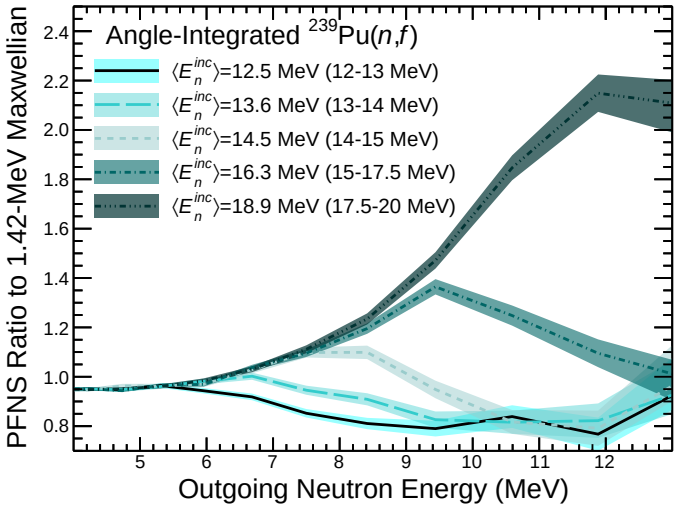

FIG. 2: (color online) The energy dependence of fission neutrons in ^{239}Pu(n,f) is shown. The various line styles and shades of blue describe the PFNS for incident neutron energy ranges in which pre-equilibrium pre-fission neutrons are observed. Average incident neutron energies, $\langle E_n^{inc}\rangle$, over the plotted range are also specified. The width of each distribution reflects the statistical uncertainties in the measured spectrum. All spectra were scaled to have the same integral from in the 3–5 MeV outgoing neutron energy range.

these neutrons has ever been carried out. Furthermore, some past experiments that inform fission models on this process were not tagged on nuclear fission events [8, 11]. Even recent experiments to measure the ^{239}Pu and ^{238}U PFNS [12, 13] have assumed that their reported results are insensitive to the pre-fission pre-equilibrium component of the PFNS, but there is no experimental evidence to support or refute this claim. In terms of fission modeling efforts, Maslov *et al.* [14], Rubchenya [15], the FREYA code [16], the CGMF code [17], and recent evaluations using the Los Alamos Model [3, 18–20] all use the exciton model [5, 21, 22] to describe the energy distribution of pre-equilibrium neutrons. This model inherently *does not predict angular distributions*, though Rubchenya [15] used a Kalbach-Mann (K-M) [23] angular distribution in conjunction with the exciton model to attempt to describe the angular effects. The inability of this model to predict the angular dependence of pre-equilibrium processes calls into question the capability of this model to reproduce the angle-integrated energy dependence of pre-equilibrium pre-fission neutrons. However, the wide use of the exciton model suggests some belief that angle-integrated energy distributions are capable of describing experimental data. This belief appears to be supported by recently-published preliminary PFNS results [24]. The model of Feshbach, Kerman, and Koonin (FKK) [25] was used by Kawano *et al.* [11] to describe the angle- and energy-dependent features of the total pre-equilibrium spectrum of ^{238}U with extensions to the impact on the PFNS, but the simplistic assumptions in that method (discussed towards the end of this work) leave questions about the applicability of their method [14]. This publication documents the first experimental measurement of the pre-equilibrium component of the ^{239}Pu(n,f) PFNS and the first continuous fission-tagged double-differential measurement of pre-equilibrium pre-fission neutrons for *any* nucleus.

The Los Alamos Neutron Science Center at Los Alamos National Laboratory houses the Chi-Nu experiment to measure the PFNS of major actinides [26, 27]. Details of the Chi-Nu experimental setup and data analysis techniques can be found in Refs. [24, 26, 28–30], and so only the essential details will be repeated here. The neutron spectra analyzed in this paper were measured with an array of 54 liquid scintillator detectors placed at angles corresponding to the surface of a hemisphere at a target-to-detector distance of $\approx$ 1 m with an actinide-containing parallel-plate avalanche counter target [31]. All neutrons used to calculate the spectra shown here were measured to be in coincidence with a fission event.

A series of tests validating the observation of the pre-fission pre-equilibrium component of the PFNS via comparisons against the expected behavior were carried out, and are summarized in Figs. 2, 3, and 4. The acquired spectra, shown in Fig. 2 as a function of incident neutron energy, show a clear excess of counts that evolves towards higher outgoing neutron energies with increasing incident neutron energy. This behavior is consistent with the expected behavior of pre-equilibrium neutron spectra [32, 33]. Also, the peak of the excess appears to be shifted downward with respect to the incident neutron energy by approximately the fission binding energy ($\approx$ 6 MeV), as expected for pre-fission pre-equilibrium neutron spectra [4]. Figure 3 shows the behavior of the excess observed for an incident energy range

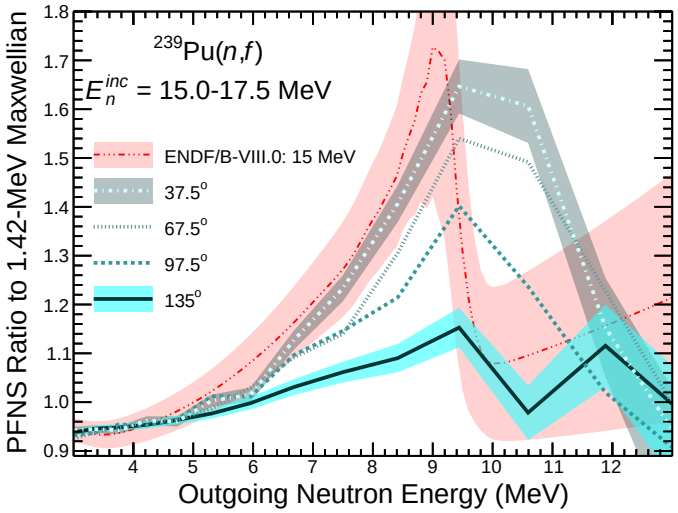

FIG. 3: (color online) The angular dependence of the fission neutron spectrum of ^{239}Pu(n,f) is shown. Lines of different styles and shades of blue correspond to different detection angles. The width of the largest and smallest angles represents the statistical uncertainty. The uncertainties for the intermediate angles are not shown but are similar. The ENDF/B-VIII.0 [3] PFNS at E_n^{inc} = 15 MeV is shown as the red dash-triple-dotted line and shaded region, the latter of which represents the evaluation uncertainty. Note that the pre-equilibrium neutrons are clearly observed even at angles above 90°. All spectra were scaled to have the same integral in the 3–5 MeV outgoing neutron energy range.

of E_n^{inc} = 15.0-17.5 MeV as a function of detection angle compared to the ENDF/B-VIII.0 [3] evaluated PFNS for E_n^{inc} = 15 MeV. Note that the ENDF/B-VIII.0 spectra are not differentiated by angle and are assumed to be integrated over all observable angles. The onset energy of this PFNS feature appears consistent with the ENDF/B-VIII.0 prediction, further suggesting that this feature is the pre-equilibrium pre-fission component of the PFNS. Additionally, Fig. 3 demonstrates the observation of the expected forward-peaked angular distribution with respect to the momentum direction of the incident neutron beam, which is not to be confused with the orientation of the fission axis.

The strongly-anisotropic character of the pre-equilibrium pre-fission neutrons implies that the observed PFNS should be harder (i.e., higher average PFNS energy) at forward (small) angles than it is at backward (large) angles once pre-equilibrium neutron emission is present. This effect is shown in Fig. 4 through the ratio of the average PFNS energy at the minimum detection angle to that of the maximum detection angle for an outgoing PFNS energy range in which largely isotropic, post-fission neutrons are expected to dominate (E_n^{out} = 1–3 MeV; blue, open circles) and for a range including the higher outgoing PFNS energies where the anisotropic pre-equilibrium pre-fission neutrons are expected to become significant (E_n^{out} = 1–12 MeV; black diamonds). This hardening of the PFNS begins at $E_n^{inc} \approx 12$ MeV, and becomes more impactful with increasing incident neutron energy, while the average PFNS energy for the lower outgoing energy range is consistent with unity for all incident energies. The mean energy ratios that contain the pre-equilibrium pre-fission PFNS component shown in Fig. 4 stop increasing after E_n^{inc} = 16–17 MeV because the high-energy tail of this neutron excess begins to go outside of the dynamic range for the detectors used in this experiment (see Fig. 2). If the entire excess were measured, this trend is expected continue upwards, possibly reaching 9–10% at E_n^{inc} = 20 MeV, which is enough to significantly distort PFNS-based calculations as a function of angle. The evidence shown in Figs. 2, 3, and 4 validate the conclusion that this feature is the pre-equilibrium pre-fission component of the PFNS, observed clearly from neutron-induced fission of ^{239}Pu for the first time and observed as a continuous fission-tagged function of incident neutron energy, outgoing neutron energy, and outgoing neutron detection angle for the first time for any target nucleus.

The counts within the pre-equilibrium excess shown in Figs. 2 and 3 that are observed above the underlying post-fission PFNS can be extracted like a peak above a background. This has not been done in past experiments because the statistical precision for neutrons in coincidence with fission and the angular coverage of the present experiment were not reached. The post-fission neutron spectrum underlying the pre-equilibrium neutron excess was characterized via a Watt distribution [34] for each incident neutron energy and detection angle and removed from the total spectrum, yielding the number of counts in the pre-equilibrium excess. These counts were then used in a calculation of the double-

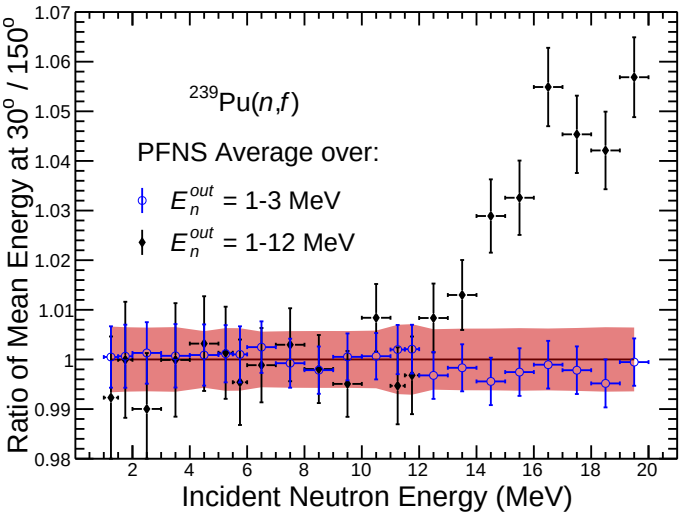

FIG. 4: (color online) The ratios of the average PFNS energy over an outgoing range of E_n^{out} = 1–3 MeV (blue, open circles) and E_n^{out} = 1–12 MeV (black diamonds) at a detection angle of 30° to the same quantity calculated at 150° as a function of incident neutron energy are shown. The uncertainties on the data points represent the uncertainty on the mean energy at 30° while the width of the shaded region around a ratio of unity (red online) represents the uncertainty of the mean energy at 150°for E_n^{out} = 1–12 MeV. See the text for discussion.

differential cross section shape for pre-equilibrium pre-fission neutrons by applying corrections for neutron detection efficiency and environmental scatter effects using MCNP®6 [35], and also for the number of observed fission events in each incident energy range, which includes details of the beam flux, fission detection efficiency, target density, and other experimental effects. The covariances associated with this method were propagated in the usual manner. The details of this calculation and propagation of the associated covariances will be described in a forthcoming publication [36]. The results of this analysis are shown as the black data points in Fig. 5. A clear, increasing trend towards smaller (more forward) angles is observed in every incident energy range. Two model comparisons were made with the results in Fig. 5: first, a K-M [23] fit to the experimental data was performed, and second, the predicted angular distribution from FKK [11, 25] was compared to the data. The K-M systematics description of continuum angular distributions is written as

$$\frac{d^2\sigma}{d\Omega dE} = \sigma_{\rm MSD}\sum_{l=0}^{l_{max}} b_l P_l(\cos\theta) + \sigma_{\rm MSC}\sum_{l=0,\Delta l=2}^{l_{max}} b_l P_l(\cos\theta), \quad (1)$$

where $\sigma_{\rm MSD}$ and $\sigma_{\rm MSC}$ are the cross sections for multi-step direct and multi-step compound process, the $P_l(\cos\theta)$ are the Legendre polynomials, and the b_l are the contributions of each Legendre polynomial to the cross section. Since we are exclusively measuring pre-equilibrium neutrons, which do not proceed via compound reactions, we set $\sigma_{\rm MSC}$ to 0. Furthermore, since we obtain a double differential cross section shape from the counts in the pre-equilibrium excess, the value of $\sigma_{\rm MSD}$ resulting from each K-M fit contains the true multi-step direct cross section as well as experimental parameters that could not be independently isolated. For this reason, we do not report values of $\sigma_{\rm MSD}$ resulting from the fits and instead show shape comparisons to the experimental data.

To determine the maximum required Legendre polynomial l value to describe the data, l_{max}, a statistical F-test was carried out for the comparisons of each increasing l_{max} [37]. The results of these fits are shown as the shaded regions of Fig. 5. Fits with l_{max} = 2 are shown as the red shaded region, which was the maximum required l_{max} to describe the data for most of the incident energy ranges reported here. However, E_n^{inc} = 15–16 MeV and 16–17 MeV were better described by an l_{max} = 3 K-M fit, and so these fits are shown as the cyan shaded regions in Figs. 5(b) and 5(c). The spread in the shaded region represents the 1-σ uncertainties of the K-M fit, obtained from the 0.16 and 0.84 quantiles of a Monte Carlo variation of the fit parameters within their uncertainties and considering correlations between them. We do not see sufficient evidence to interpret the improved fit quality obtained using l_{max} = 3 for

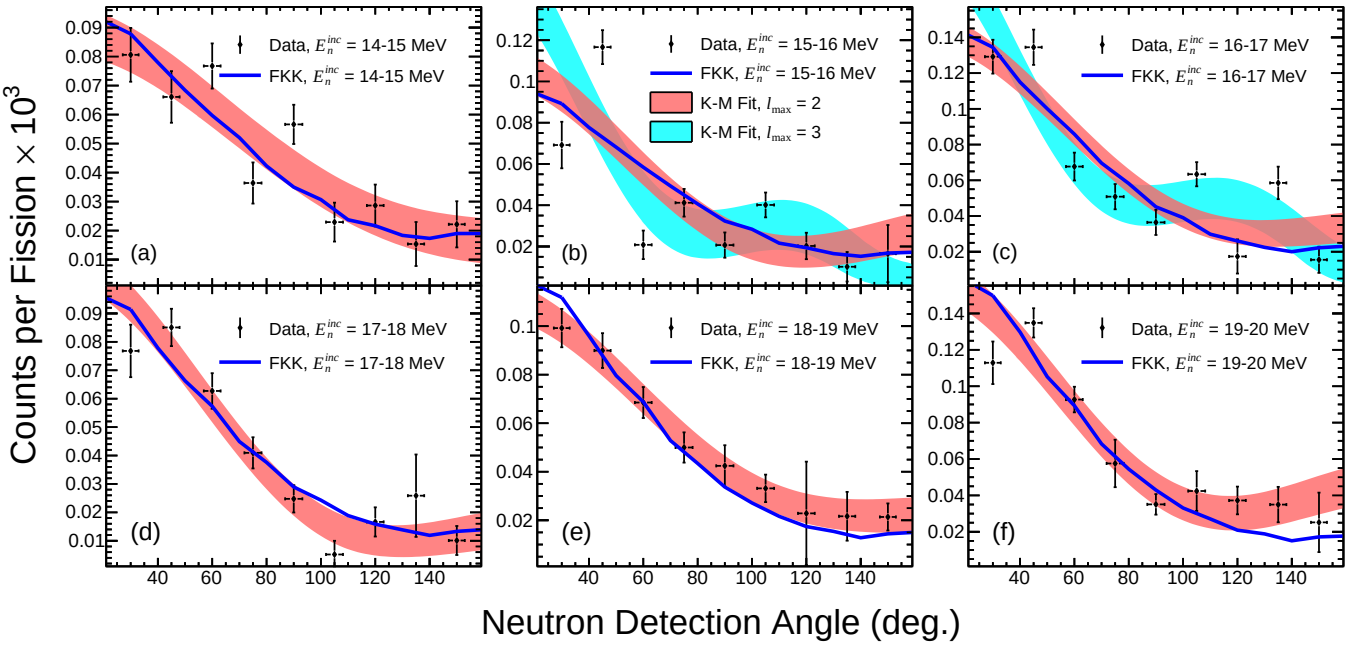

FIG. 5: (color online) The angular distributions of counts in the pre-equilibrium pre-fission neutron excess region in ^{239}Pu(n,f) are shown as black diamonds. The red and cyan shaded regions are K-M fits to the experimental data with $l_{max} = 2$ and 3, respectively as indicated on panel (b), and the widths of the distributions include the model uncertainties and parameter correlations from the fit. The solid, blue lines are FKK predictions for the angular distributions calculated following Ref. [11] averaged over the lower and upper limits of the incident energy range shown on each plot. The statistical scatter of the data is reduced with increasing incident neutron energy because the effect of pre-equilibrium neutron emission is larger at higher incident energies. Note that the angles shown on the x axis are defined with respect to the momentum direction of the incident neutron.

the data shown in Figs. 5(b) and 5(c) as an indication of new physics. Instead, this improved fit quality is likely the result of the increased statistical scatter of the experimental data in Figs. 5(b) and 5(c) combined with the additional free parameter available in the $l_{max} = 3$ fit. Nonetheless, the optimal l_{max} from each fit as indicated by each F-test is included in Figs. 5(a)–5(f) to avoid any bias in the presentation of these results. The K-M systematics appear to be able to describe the angular trends in the data, indicating that this theory is still applicable for the observed pre-equilibrium pre-fission neutrons despite the lack of a fission axis specification.

The FKK predictions of ^{239}Pu were calculated following the method outlined in Ref. [11]. In that work, the pre-equilibrium neutron spectrum associated with fission was calculated assuming that all inelastic scattering events that leave the target actinide with an excitation energy above the fission barrier height, B_f, produce a fission event. So, the fission-correlated pre-equilibrium neutron spectrum was simply the spectrum of neutrons below the energy $E = E_n^{inc} - B_f$. The angular distribution of neutrons within the same pre-equilibrium excess region identified in the data was calculated for the relevant incident neutron energy ranges, and is plotted in Fig. 5 as the solid, blue lines. Given that the results shown here are not an absolute cross section, these trends were scaled to allow for a shape comparison between the data and model prediction. The FKK prediction agrees quite well with the data, and is nearly equivalent to $l_{max} = 2$ K-M fit to the data for most angles. We therefore conclude that the FKK approach appears to be applicable to pre-equilibrium pre-fission neutron angular distributions. This result reaffirms the original, unconfirmed assumption that pre-equilibrium pre-fission neutrons are likely not correlated with the fission axis, thereby allowing for pure scattering theories to be applied.

The data shown in Fig. 5 represent the first fission-tagged double-differential measurement of pre-equilibrium pre-fission neutrons. This information will be valuable to fission models, like the Los Alamos Model, and to codes used to describe nuclear fission, such as FREYA and CGMF, for descriptions of the PFNS as a function of angle, which will in turn be used to validate and guide calculations of nuclear systems. For the impact on past experiments, the ^{239}Pu(n,f) PFNS measurement of Chatillon *et al.* [12, 38] and the ^{238}U(n,f) PFNS measurement of Ethvignot *et al.* [13] were claimed to be largely insensitive to the pre-equilibrium component of the PFNS because the minimum angles of neutron detection were 45° and 90°, respectively. However, the data shown in Fig. 5 prove that the pre-

equilibrium pre-fission component of the PFNS exists even at detection angles as large as 120°, though the statistical precision of the data from Refs. [12] and [13] did not allow for this PFNS feature to be resolved in the data. This observation alters the interpretation of Refs. [12] and [13], and likely other PFNS measurements even if detection angles were specifically chosen to be insensitive to the pre-equilibrium component of the neutron spectrum. Future fission models will be required to incorporate the angular dependence of pre-equilibrium pre-fission neutrons described here, as well as a reinterpretation of relevant literature PFNS results.

This work was performed under the auspices of the U.S. Department of Energy by Los Alamos National Laboratory under Contract DE-AC52-06NA25396 and by Lawrence Livermore National Security, LLC under contract DE- AC52-07NA27344.

[1] M. Aufiero, G. Palmiotti, M. Salvatores, and S. Sen, Ann. Nucl. Energy **98**, 218 (2016).
[2] M. B. Chadwick, M. Herman, P. Oblŏzinský, M. E. Dunn, Y. Danon, *et al.*, Nucl. Data Sheets **112**, 2887 (2011).
[3] D. A. Brown, M. B. Chadwick, R. Capote, A. C. Kahler, A. Trkov, *et al.*, Nucl. Data Sheets **148**, 1 (2018).
[4] R. Capote, Y.-J. Chen, F.-J. Hambsch, N. V. Kornilov, J. P. Lestone, *et al.*, Nucl. Data Sheets **131**, 1 (2016).
[5] E. Gadioli and P. E. Hodgson, *Pre-equilibrium Nuclear Reactions* (Oxford University Press, New York, 1992).
[6] J. L. Kammerdiener, *Neutron Spectra Emitted by* ^{239}*Pu,* ^{238}*U,* ^{235}*U, Pb, Nb, Ni, Al, and C Irradiated by 14 MeV Neutrons*, Ph.D. thesis, University of California/Lawrence Livermore National Laboratory (1972).
[7] N. V. Kornilov, V. J. Baryba, and O. A. Sal'nikov, All Union Conf. on Neutron Phys., Kiev **3**, 104 (1980).
[8] M. Baba, H. Wakabayashi, N. Ito, K. Maeda, and N. Hirakawa, J. Nucl. Sci. Technol. **27**, 7 (1990).
[9] G. Boykov, V. Dmitriev, G. Kudyaev, Y. Ostapenko, M. Svirin, *et al.*, IAEA Consult. Meet. on "Nuclear Data for Neutron Emission in the Fission Process", Vienna, 22–24 October 1990, Report **INDC(NDS)-251**, IAEA, Vienna, Austria, 189 (1991).
[10] G. N. Lovchikova, A. M. Trufanov, M. I. Svirin, and V. A. Vinogradov, Yad. Fiz. **67**, 914 (2004).
[11] T. Kawano, T. Ohsawa, M. Baba, and T. Nakagawa, Phys. Rev. C **63**, 034601 (2001).
[12] A. Chatillon, G. Bélier, T. Granier, B. Laurent, B. Morillon, *et al.*, Phys. Rev. C **89**, 014611 (2014).
[13] T. Ethvignot, M. Devlin, R. Drosg, T. Granier, R. C. Haight, *et al.*, Phys. Lett. B **575**, 221 (2003).
[14] V. M. Maslov, Y. V. Porodzinskij, M. Baba, A. Hasegawa, N. V. Kornilov, *et al.*, Phys. Rev. C **69**, 034607 (2004).
[15] V. A. Rubchenya, Phys. Rev. C **75**, 054601 (2007).
[16] R. Vogt, J. Randrup, D. A. Brown, M. A. Descalle, and W. E. Ormand, Phys. Rev. C **85**, 024608 (2012).
[17] P. Talou, R. Vogt, J. Randrup, M. E. Rising, S. A. Pozzi, *et al.*, Eur. Phys. J. A **54**, 9 (2018).
[18] O. Iwamoto, J. Nucl. Sci. Tech. **45 9**, 910 (2012).
[19] G. Vladuca and A. Tudora, Ann. Nucl. Energy **28**, 419 (2001).
[20] D. Neudecker, P. Talou, T. Kawano, A. Kahler, M. White, *et al.*, Nucl. Data Sheets **148**, 293 (2018).
[21] J. Dobeš and E. Běták, Z. Phys. **A310**, 329 (1983).
[22] A. J. Koning and M. C. Duijvestijn, Nucl. Phys. A **744**, 15 (2004).
[23] C. Kalbach and F. M. Mann, Phys. Rev. C **23**, 112 (1981).
[24] K. J. Kelly, J. A. Gomez, J. M. O'Donnell, M. Devlin, R. C. Haight, *et al.*, Proceedings of the 20th Topical Meeting of the Radiation Protection and Shielding Division (2018).
[25] H. Feshbach, A. Kerman, and S. Koonin, Ann. Phys. (N.Y.) **125**, 429 (1980).
[26] M. Devlin, J. A. Gomez, K. J. Kelly, R. C. Haight, J. M. O'Donnell, *et al.*, Nucl. Data Sheets **148**, 322 (2018).
[27] K. J. Kelly, M. Devlin, J. A. Gomez, J. M. O'Donnell, T. N. Taddeucci, *et al.*, EPJ Web of Conferences **193**, 03003 (2018).
[28] R. C. Haight, C. Y. Wu, H. Y. Lee, T. N. Taddeucci, B. A. Perdue, *et al.*, Nucl. Data Sheets **123**, 130 (2015).
[29] T. N. Taddeucci, R. C. Haight, H. Y. Lee, D. Neudecker, J. M. O'Donnell, *et al.*, Nucl. Data Sheets **123**, 135 (2015).
[30] K. J. Kelly, J. M. O'Donnell, J. A. Gomez, T. N. Taddeucci, M. Devlin, *et al.*, Nucl. Instrum. and Methods A **866**, 182 (2017).
[31] C. Y. Wu, R. A. Henderson, R. C. Haight, H. Y. Lee, T. N. Taddeucci, *et al.*, Nucl. Instrum. and Methods A **794**, 76 (2015).
[32] J. J. Griffin, Phys. Rev. Lett. **17**, 478 (1966).
[33] K. Cline and M. Blann, Nucl. Phys. A **172**, 225 (1971).
[34] B. E. Watt, Phys. Rev. **87**, 1037 (1952).
[35] J. Armstrong, F. B. Brown, J. S. Bull, L. Casswell, L. J. Cox, *et al.*, LA-UR-17-29981 (2017).
[36] K. J. Kelly, M. Devlin, J. A. Gomez, J. M. O'Donnell, R. C. Haight, *et al.*, Phys. Rev. C **In Preparation**.
[37] P. Bevington and D. K. Robinson, *Data Reduction and Error Analysis for the Physical Sciences, Third Edition* (McGraw Hill Education, 2003).
[38] T. Granier, Phys. Proc. **64**, 183 (2015).